



# Exploring Brain Function-Structure Connectome Skeleton via Self-supervised Graph-Transformer Approach

Yanqing Kang, Ruoyang Wang, Enze Shi, Jinru Wu, Sigang Yu, and Shu Zhang<sup>(✉)</sup>

Center for Brain and Brain-Inspired Computing Research, School of Computer Science,  
Northwestern Polytechnical University, Xi'an, China  
shu.zhang@nwpu.edu.cn

**Abstract.** Understanding the relationship between brain functional connectivity and structural connectivity is important in the field of brain imaging, and it can help us better comprehend the working mechanisms of the brain. Much effort has been made on this issue, but it is still far from satisfactory. The brain transmits information through a network architecture, which means that the regions and connections of the brain are significant. The main difficulties with this issue are currently at least two aspects. On the one hand, the importance of different brain regions in structural and functional integration has not been fully addressed; on the other hand, the connectome skeleton of the brain, plays the role in common and key connections in the brain network, has not been clearly studied. To alleviate the above problems, this paper proposes a transformer-based self-supervised graph reconstruction framework (TSGR). The framework uses the graph neural network (GNN) to fuse functional and structural information of the brain, reconstructs the brain graph through a self-supervised model and identifies the regions that are important to the reconstruction task. These regions are considered as key connectome regions which play an essential role in the communication connectivity of the brain network. Based on key brain regions, the connectome skeleton can be obtained. Experimental results demonstrate the effectiveness of the proposed method, which obtains key regions and connectome skeleton in the brain network. This provides a new angle of view to explore the relationship between brain function and structure. Our code is available at <https://github.com/kang105/TSGR>.

**Keywords:** Brain Function · Brain Structure · Self-supervised · Graph Neural Network · Transformer

## 1 Introduction

Understanding the relationship between brain functional connectivity and structural connectivity is a key issue in studying the working mechanisms of the brain [1, 2]. In the early stage, due to the dynamic variability nature of functional connectivity and the unique stability of structural connectivity, the two were often analyzed separately [3, 4]. Later,

attention was paid to their relationship, and a large number of studies were proposed to analyze this issue [5–7]. For example, Greicius *et al.* [5] found that higher structural connectivity tended to be accompanied by higher functional connectivity; MIŠIĆ *et al.* [6] used a multimodal approach to correlate structural and functional connectivity with each other using partial least squares analysis while searching for the best covariance pattern of both; Sarwa *et al.* [7] adopted a deep learning framework for structural connectivity to functional connectivity prediction.

Despite the great success of the above methods, they are far from satisfactory for studying the relationship between brain functional and structural connectivity. Connections in brain regions make up networks, and it is crucial to identify key nodes and connections. Therefore, there are currently at least two difficulties. On the one hand, key brain regions, act as hubs for information transmission in the brain network, have not been completely identified in the joint analysis of brain functional and structural profiles. On the other hand, it has not been clearly studied for the connectome skeleton of brain, which plays a key role in both functional and structural connections of brain.

To overcome the above limitations, we propose a transformer-based graph self-supervised graph reconstruction framework. It can obtain the key connectome regions and skeleton of brain by combining brain function and structure. The method has two main characteristics. For one thing, graph neural networks (GNN) [8] is applied to integrate brain function and structure. We represent the brain as a graph, which its nodes are the regions of interest (ROIs) defined by the atlas. The edge information and node features of the graph come from the structural connectivity and the functional connectivity of the ROIs, respectively. The graph features are propagated through the self-attention mechanism [9] and graph convolution network (GCN) [10]. For the other thing, a self-supervised model is adopted to reconstruct the brain graph and obtain the contribution scores of ROIs for the reconstruction task. ROIs with higher scores are more important for reconstruction and are considered as key connectome regions of brain. We used several functional magnetic resonance imaging (fMRI) from the Human Connectome Project (HCP) 900 datasets [11], combined them with structure connectivity from diffusion-weighted MRI (dMRI) separately, and acquired the corresponding key connectome regions. Based on key regions, we obtained the connectome skeleton of the brain.

Experimental results demonstrate the effectiveness of proposed method. First, we obtained low loss values, which indicated that the model achieved the reconstruction task. Second, we obtained the contribution scores of brain ROIs. ROIs with high scores play a role in the transmission of information in the network, are regarded as key connectome regions. Finally, we obtained the connectome skeleton of the brain, which expresses the most key connections of the brain both in functional and structural networks.

## 2 Method

### 2.1 Overview

The pipeline of the transformer-based self-supervised graph reconstruction (TSGR) framework proposed in this paper is shown in Fig. 1. The method analyzes key connectome regions of brain in the joint analysis of brain functional and structural profiles.

The brain is represented as a graph and used as input for the ScorePool-AE module, then the reconstructed graph and contribution scores of the nodes can be obtained. The framework consists of three main parts, i.e., graph generation, ScorePool-AE module, and reconstruction target. In the graph generation part, we adopt Destrieux Atlas to initialize the brain surface into 148 ROIs and use them as nodes of the graph. Based on the ROIs, functional and structural information are utilized to generate the node features and edge features of the graph, respectively. In the ScorePool-AE module, we design ScorePool to get the contribution score of each node in the graph. In the reconstruction target part, the mean square error (MSE) between the node features of the input graph and the reconstructed graph is applied as the loss function.

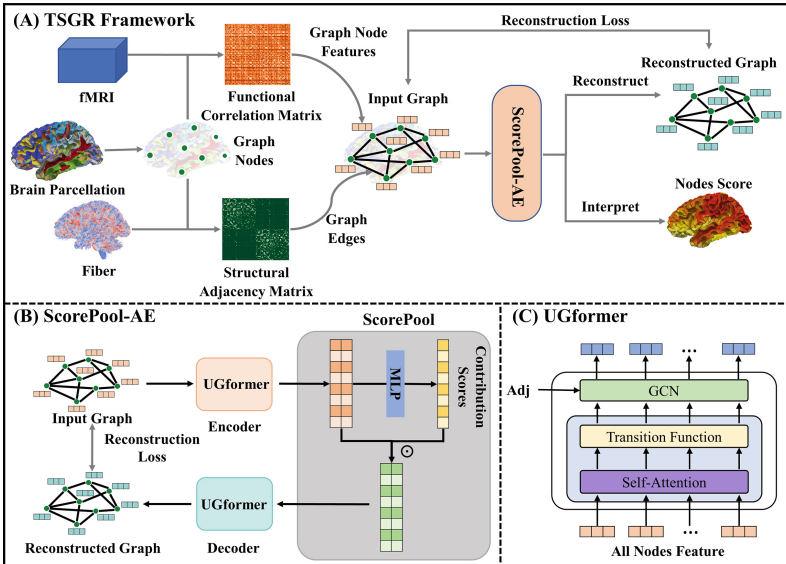


**Fig. 1.** The pipeline of the proposed TSGR framework. (A) represents the process of the framework, including three parts, i.e., graph generation, ScorePool-AE module, and reconstruction target. (B) represents the ScorePool-AE module architecture. (C) represents the UGformer.

## 2.2 Data and Preprocess

We used the HCP 900 dataset and randomly selected 98 subjects from it. T1-weighted MRI data were used to reconstruct the brain cortical surface, dMRI were utilized to reconstruct the fiber bundles from white matter, resting-state fMRI (rs-fMRI) and task fMRI showed the functional changes of the brain. Among them, task fMRI data contains a total of seven tasks, which are EMOTION, GAMBLING, LANGUAGE, MOTOR, RELATION, SOCIAL and WM.

Standard Freesurfer pipeline including tissue-segmentation and white matter surface (inner surface) reconstruction [12] is proposed to preprocess the T1-weighted MRI. For rs-fMRI, we adopted the gray coordinate system [13] as the platform to extract rs-fMRI

time sequence for each surface vertex. For dMRI, we followed the method in Van den Heuvel *et al.* [14] to use deterministic tractography to derive white matter fibers, and reconstructed  $5 \times 10^4$  fiber tracts for each subject.

To jointly use these three modalities, we aligned them into the same space. A linear image registration method (FLIRT) [15] and a nonlinear one (FNIRT) [16] were cascaded to transform and warp T1-weighted MRI to the dMRI space. The preprocessed rs-fMRI uses gray coordinate system, which is located at the same space as T1-weighted MRI, and the vertex-wise correspondence between them can be directly established.

### 2.3 TSGR Framework

**Graph Generation.** We define the brain as an undirected graph  $G = \{V, E\}$ .  $V = \{v_i | i \in 1, 2, \dots, n\}$  represents the set of nodes of the graph.  $F \in \mathbb{R}^{n \times D}$  represents the feature matrix of graph nodes.  $E \in \mathbb{R}^{n \times n}$  represents the adjacency matrix of the graph.

*Graph Nodes with Generated Features.* The brain surface is divided into 148 ROIs and used as nodes of the graph. fMRI signals are selected to express node features. We compute the Pearson correlation coefficients of the signals among all ROIs to obtain the functional similarity matrix and use it as the feature matrix  $F$  of the graph nodes. The length of each node feature  $D$  is 148.

*Graph Edge.* For each pair of ROIs, we calculate the total number of fibers directly connected of them and then divide it by the geometric mean of their areas, thus obtaining the structural connectivity matrix  $S$ . We set the threshold  $t_s$  for  $S$  to make it sparse and do the binarization to obtain  $E$ .  $E_{i,j} = 1$  means that nodes  $i$  and  $j$  are connected, otherwise  $E_{i,j} = 0$ .

**ScorePool-AE Module.** In ScorePool-AE module, we adopt the encoder-decoder structure to implement the graph reconstruction task. The encoder is applied to extract node representations of the graph, then the ScorePool is used to obtain the contribution scores of nodes, and finally the decoder is used to reconstruct the node features of the graph.

The encoder is based on the Ugformer [17], which implements the self-attention mechanism on the nodes of the graph via transformer. For one of the layers of UGformer, the self-attention mechanism is adopted on all nodes of the graph rather than on neighboring nodes, then GCNs is applied to exploit the structural information of the graph. The process is shown as Eq. (1) and (2).

$$H'^{(k)} = \text{Attention}_V \left( H^{(k)} Q^{(k)}, H^{(k)} K^{(k)}, H^{(k)} V^{(k)} \right) \quad (1)$$

$$H^{(k+1)} = \text{GCN} \left( E, H'^{(k)} \right) \quad (2)$$

where  $H^{(k)}$  is the node representations of the graph at the  $k$ -th layer of UGformer.  $V$  is the set of all nodes of the graph.  $Q^{(k)}, K^{(k)}, V^{(k)} \in \mathbb{R}^{d_0 \times d}$  are the projection matrices.

Inspired by the pooling operation of the GNN [18], we design the ScorePool to get the contribution score of each node in the graph for the reconstruction task. ScorePool comes after encoder and before decoder. The output of encoder is the graph node representations  $X \in \mathbb{R}^{n \times d}$ , which is used as the input of the ScorePool. After an MLP layer,  $X$  is mapped

to  $Y \in \mathbb{R}^{n \times 1}$ .  $Y$  is seen as the scores of graph nodes. Finally, we do the element-wise product operation of  $X$  and  $Y$ , and use it as the input of the decoder. It is calculated as Eqs. (3) and (4). The decoder has the same structure as the encoder and is utilized to reconstruct the node features.

$$Y = \text{softmax}(\text{MLP}(X)) \quad (3)$$

$$X' = X \odot Y \quad (4)$$

where  $\odot$  denotes the element-wise product and  $X'$  denotes the input of the decoder.

**Reconstruction Target.** Our TSGR framework reconstructs the graph by predicting the nodes features of the graph. The loss function is MSE between the feature matrix  $F'$  of reconstructed graph nodes and the feature matrix  $F$  of input graph nodes.

## 2.4 Analyzing Brain Key Connectome ROIs and Hierarchical Networks

In this work, we propose a method that identifies key connectome ROIs and can be applied to the hierarchical analysis of brain networks. First, we obtained the average contribution scores of brain ROIs for all individuals. Second, we verify whether the ROIs with high scores are key connectome ROIs in the functional and structural networks. The functional network is obtained by averaging  $F$  over all individuals and setting a threshold. The structural network is the same operation done for  $S$ . We use three network centrality metrics, i.e., degree centrality, closeness centrality and PageRank centrality, to measure key connectome ROIs. In addition, we calculate the number of all ROIs participating in the functional network, where the functional networks are obtained by dictionary learning [19]. Finally, we divide all brain ROIs into 3 scales and analyze the characteristics of networks consisting of ROIs at different scales, namely, the connectivity strength and global efficiency of the networks.

## 2.5 Exploring the Connectome Skeleton of Brain ROIs

This study explores the connectome skeleton of the brain based on important ROIs. The connectome skeleton plays the role in common connections in the brain network and is a core connectivity pattern. First, we obtain the key functional connections of eight (one resting-state and seven tasks) functional networks. Specifically, we calculate the eight functional network connections consisting of Scale-1 and Scale-2 ROIs, and a connection is selected if it exists simultaneously in six and more functional networks. Then, we obtain the intersection between the key functional connections and the structural network connection as the connectome skeleton. Finally, we analyze the connectome skeleton, namely, counting the strength of connectivity between brain regions and the length of fibers in the connectome skeleton.

### 3 Experiments and Results

#### 3.1 Experimental Performance

**Experimental Setup.** A total of 98 individuals is evaluated by the proposed method. Each individual has eight brain graphs, which have the same topology corresponding to the structural information and different node features corresponding to eight kinds of functional information. We set up eight sets of experiments, each of which is trained independently. Each set of experiments use one of the brain graphs from 98 individuals, which corresponded to the same kind of functional information. These eight sets of experiments are called REST, EMOTION, GAMBLING, LANGUAGE, MOTOR, RELATION, SOCIAL and WM. We set the number of layers of the UGformer in the encoder and decoder to 1, and the number of heads in the self-attention to 4. The model is trained for 200 epochs using the Adam optimizer to update parameters.

**Reconstruction Effect.** The final loss values of experiments obtained are low. To verify the effect of reconstruction graph, we calculated Correlation and SSIM [20] between the input node features and the reconstructed node features for all individuals, as shown in Fig. 2. We find out that for all eight sets of experiments, the average Correlation and SSIM of all individuals are around 0.9997. This indicates that our method achieves the reconstruction task and we can further analyze based on experimental results.

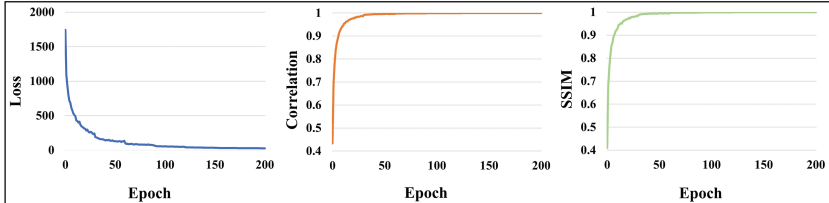


Fig. 2. Experimental performance of REST

#### 3.2 Analysis of Key Brain ROIs and Network Hierarchy

For each set of experiments, the contribution scores of brain ROIs are obtained by averaging the scores of all individuals, as shown in Fig. 3. According to the scores from high to low, we divide the ROIs into 3 scales. Each scale contains 20%, 30%, and 50% of the ROIs, and the corresponding number of ROIs is 30, 44, and 74 respectively. Scale-1 ROIs are considered as key connectome ROIs. Scale-2 and Scale-3 are in descending order of importance in brain connectivity.

Figure 3(B) shows Scale-1 ROIs in eight sets of experiments, which are basically distributed in the superior frontal, parietal, and occipital of the lateral brain, with little distribution in the medial and bottom parts of the brain. These regions have important biological significance, for example, Heuvel *et al.* confirmed that the parietal and prefrontal cortex contain multiple hubs in almost all species [21]. Figure 3(D) lists the Scale-1

specific ROIs for all experiments. Some ROIs exist in the Scale-1 of most experiments, such as the F\_mid, Precentral, and O\_mid, indicating that these ROIs are involved in the functional network of multiple tasks; some ROIs are unique to one experiment, such as the fronto-margin only in the SOCIAL, indicating that this ROI is more important in this task. Figure 3(C) shows the Scale-1 IoU in all experiments, and it can be seen that EMOTION and LANGUAGE have the highest value, indicating that the functional activation of these two tasks is similar.

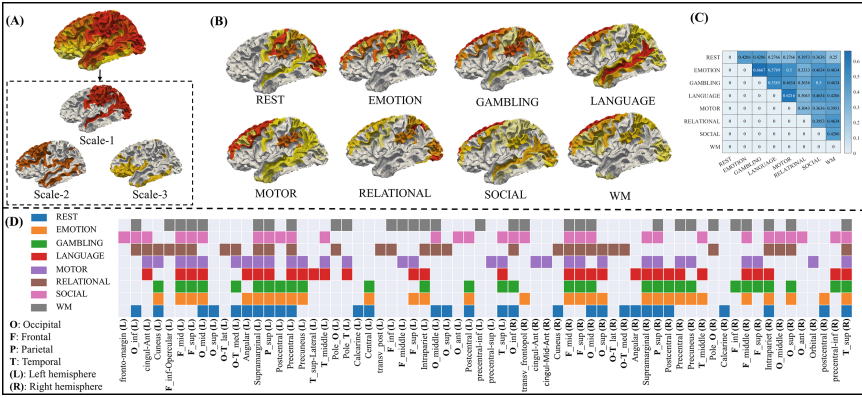


**Fig. 3.** Visualization of contribution scores of brain ROIs. (A) represents the scores of all ROIs and division of ROIs at REST. (B) and (D) show the Scale-1 ROIs in all experiments. (C) shows the IoU of the Scale-1 ROIs in all experiments.

To verify whether the ROIs with high scores are key connectome ROIs, we calculate the centrality of all ROIs in the functional network (orange) and structural network (green) separately, and the horizontal axis indicates the ROIs ranked from lowest to highest scores, as shown in Fig. 4(A). Here we use three centrality metrics, namely degree centrality, closeness centrality, and PageRank centrality. The results show that the metrics are positively correlated with scores of ROIs. We also calculate the number of all ROIs participating in the functional network (purple), and the results are positively correlated with scores of ROIs. This indicates that ROIs with high scores are located in key positions at the network and participate in more functional networks.

In addition, we also investigate the networks composed among the scales. As shown in Fig. 4(B), the functional and structural connectivity strength is relatively similar overall, with decreasing strength of connections in the Scale-1, Scale-2 and Scale-3. We also analyze the global efficiency of the network and the coupling between the functional and structural networks, as shown in Fig. 4(C). Among the functional and structural networks, S1\_1 has the highest global efficiency for most of the experiments, followed by S1\_2 and S2\_2. It can be seen at the bottom of Fig. 4(C), S1\_1 has the highest functional-structural coupling. Therefore, we consider the Scale-1 ROIs as key connectome ROIs, and the network they form assumes the main information transfer function in the functional and structural network.

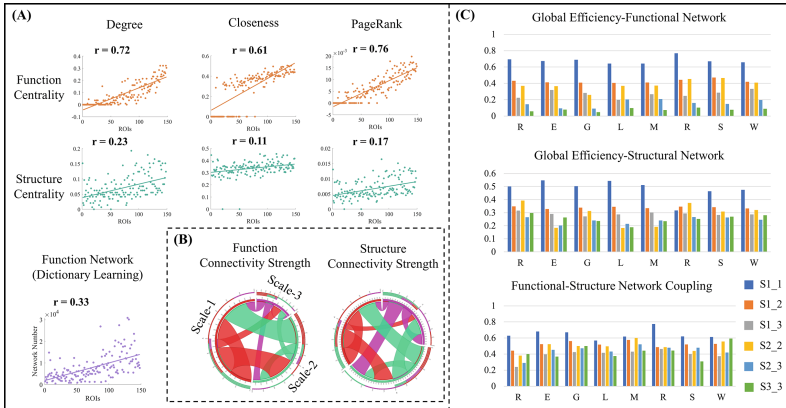


**Fig. 4.** Analysis of key ROIs and hierarchical network. (A) represents the centrality of all ROIs in the functional and structural networks, and the number of ROIs participating in the functional network in the REST. (B) represents the functional and structural connectivity strength among the 3 scales in the REST. (C) represents the analysis of the network composed among the 3 scales.

### 3.3 Analysis of Connectome Skeleton in Brain Networks

We obtain the key connection for the functional network of all eight functional networks, where the functional network consists of connections within the ROIs including Scale-1 and Scale-2. Then we combine the key functional connections and the structural connections to obtain the connectome skeleton, as shown in Fig. 5(A).

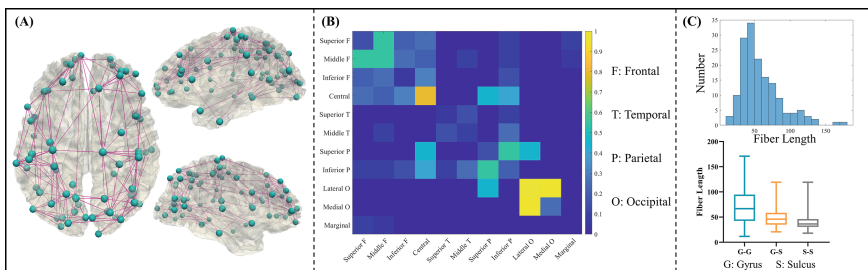


**Fig. 5.** Analysis of connectome skeleton. (A) represents the visualization of the connectome skeleton. (B) and (C) represents the distribution of connectome skeleton in brain regions and fiber length, respectively.

It shows that the connections are distributed more evenly over the whole brain rather than concentrated in a particular region. From Fig. 5(B), it can be concluded that the intra-occipital and intra-central connections are the most numerous, while the frontal and parietal connections are more evenly distributed. This indicates that the occipital region plays an important role in the connectome skeleton. We count the fiber lengths in the connectome skeleton, as shown in the upper of Fig. 5(C). The fiber lengths are mostly concentrated around 50 mm, and long fibers (fiber lengths greater than 80 mm) account

for about 20%, which are more distributed in the frontal region. The high percentage of short fibers improves communication efficiency. The bottom of Fig. 5(C) counts the fiber lengths of the connectome skeleton in the Gyrus-Sulcus connection, in which the fibers of the G-G connection are the longest, followed by the G-S and finally the S-S, which indicates that the connectome skeleton still follows the traditional Gyrus-Sulcus connection pattern [22, 23].

## 4 Conclusion

We propose a new transformer-based self-supervised graph reconstruction framework to identify key brain connectome ROIs and connectome skeleton in the joint analysis of brain functional connectivity and structural connectivity. The main contribution of the approach is the use of GNN to fuse brain function and structure and the use of a self-supervised model to identify the ROIs that important for graph reconstruction. The experimental results validate the effectiveness of the method. First, we obtain the scores of ROIs. Second, we verify that the ROIs with high scores are key connectome ROIs. Finally, we obtain the connectome skeleton of the brain. It provides a new approach for analyzing the relationship between functional and structural connectivity, and further analysis will be settled in future work.

**Acknowledgement.** This work was supported by the National Natural Science Foundation of China (62006194).

## References

1. Sporns, O., Tononi, G., Kötter, R.: The human connectome: a structural description of the human brain. *PLoS Comput. Biol.* **1**, e42 (2005)
2. Biswal, B., Zerrin Yetkin, F., Haughton, V.M., Hyde, J.S.: Functional connectivity in the motor cortex of resting human brain using echo-planar mri. *Magn. Reson. Med.* **34**, 537–541 (1995)
3. Zamora-López, G., Zhou, C., Kurths, J.: Cortical hubs form a module for multisensory integration on top of the hierarchy of cortical networks. *Front. Neuroinform.* **4**, 1 (2010)
4. Gordon, E.M., et al.: Precision functional mapping of individual human brains. *Neuron* **95**, 791–807.e7 (2017)
5. Greicius, M.D., Supekar, K., Menon, V., Dougherty, R.F.: Resting-state functional connectivity reflects structural connectivity in the default mode network. *Cereb. Cortex* **19**, 72–78 (2009)
6. Mišić, B., et al.: Network-level structure-function relationships in human neocortex. *Cereb. Cortex* **26**, 3285–3296 (2016)
7. Sarwar, T., Tian, Y., Yeo, B.T.T., Ramamohanarao, K., Zalesky, A.: Structure-function coupling in the human connectome: a machine learning approach. *Neuroimage* **226**, 117609 (2021)
8. Scarselli, F., Gori, M., Tsoi, A.C., Hagenbuchner, M., Monfardini, G.: The graph neural network model. *IEEE Trans. Neural Netw.* **20**, 61–80 (2009)
9. Dosovitskiy, A., et al.: An Image is Worth 16x16 Words: Transformers for Image Recognition at Scale. arXiv preprint <http://arxiv.org/abs/2010.11929> (2021)

10. Kipf, T.N., Welling, M.: Semi-Supervised Classification with Graph Convolutional Networks. arXiv preprint <http://arxiv.org/abs/1609.02907> (2017)
11. Van Essen, D.C., et al.: The human connectome project: a data acquisition perspective. *Neuroimage* **62**, 2222–2231 (2012)
12. Fischl, B., et al.: Whole brain segmentation: automated labeling of neuroanatomical structures in the human brain. *Neuron* **33**, 341–355 (2002)
13. Glasser, M.F., et al.: The minimal preprocessing pipelines for the human connectome project. *Neuroimage* **80**, 105–124 (2013)
14. van den Heuvel, M.P., Kahn, R.S., Goñi, J., Sporns, O.: High-cost, high-capacity backbone for global brain communication. *Proc. Natl. Acad. Sci.* **109**, 11372–11377 (2012)
15. Jenkinson, M., Bannister, P., Brady, M., Smith, S.: Improved optimization for the robust and accurate linear registration and motion correction of brain images. *Neuroimage* **17**, 825–841 (2002)
16. Jenkinson, M., Beckmann, C.F., Behrens, T.E.J., Woolrich, M.W., Smith, S.M.: FSL. *NeuroImage* **62**, 782–790 (2012)
17. Nguyen, D.Q., Nguyen, T.D., Phung, D.: Universal Graph Transformer Self-Attention Networks. arXiv preprint <http://arxiv.org/abs/1909.11855> (2022)
18. Gao, H., Ji, S.: Graph U-Nets. In: Proceedings of the 36th International Conference on Machine Learning, pp. 2083–2092. PMLR (2019)
19. Mallat, S.G., Zhang, Z.: Matching pursuits with time-frequency dictionaries. *IEEE Trans. Signal Process.* **41**, 3397–3415 (1993)
20. Wang, Z., Bovik, A.C., Sheikh, H.R., Simoncelli, E.P.: Image quality assessment: from error visibility to structural similarity. *IEEE Trans. Image Process.* **13**, 600–612 (2004)
21. van den Heuvel, M.P., Sporns, O.: Network hubs in the human brain. *Trends Cogn. Sci.* **17**, 683–696 (2013)
22. Deng, F., et al.: A functional model of cortical gyri and sulci. *Brain Struct. Funct.* **219**, 1473–1491 (2014)
23. Nie, J., et al.: Axonal fiber terminations concentrate on gyri. *Cereb Cortex* **22**, 2831–2839 (2012)